Mi-2/NuRD complex function is required for normal S phase progression and assembly of pericentric heterochromatin

Jennifer K. Sims and Paul A. Wade
Laboratory of Molecular Carcinogenesis, National Institute of Environmental Health Sciences, Research Triangle Park, NC 27709

ABSTRACT **During chromosome duplication, it is essential to replicate not only the DNA sequence, but also the complex nucleoprotein structures of chromatin. Pericentric heterochromatin is critical for silencing repetitive elements and plays an essential structural role during mitosis. However, relatively little is understood about its assembly and maintenance during replication. The Mi2/NuRD chromatin remodeling complex tightly associates with actively replicating pericentric heterochromatin, suggesting a role in its assembly. Here we demonstrate that depletion of the catalytic ATPase subunit CHD4/Mi-2β in cells with a dampened DNA damage response results in a slow-growth phenotype characterized by delayed progression through S phase. Furthermore, we observe defects in pericentric heterochromatin maintenance and assembly. Our data suggest that chromatin assembly defects are sensed by an ATM-dependent intra–S phase chromatin quality checkpoint, resulting in a temporal block to the transition from early to late S phase. These findings implicate Mi-2β in the maintenance of chromatin structure and proper cell cycle progression.**

Monitoring Editor
Kerry Bloom
University of North Carolina

Received: Mar 28, 2011
Revised: May 27, 2011
Accepted: Jun 27, 2011

INTRODUCTION

DNA-templated processes in eukaryotic nuclei take place within a complex nucleoprotein assembly termed chromatin. The template for production of daughter DNA strands has been recognized since the demonstration of semiconservative replication (Meselson and Stahl, 1958). Duplication of the nongenetic information of chromosomes along with their specialized, biologically essential structures represents an additional burden to the chromosomal duplication machinery. Following passage of the replication fork, normal cell division requires maintenance of protein stoichiometry, sustaining of modification status of both protein and DNA, and assembly of higher-order chromosomal structures (Groth *et al.*, 2007b). The details of how these processes are templated and how the numerous enzymatic reactions required are coordinated remain poorly understood.

Nuclear regions that remain highly condensed throughout the cell cycle are generically termed heterochromatin. In mammals, a substantial portion of the genome is embedded within heterochromatin, which tends to be gene poor and enriched in repetitive sequence, including classic satellites and transposable elements (Henikoff, 2000). Maintenance of heterochromatic structures during mitosis requires faithful replication of all epigenetic marks, as well as association of appropriate nonhistone proteins. Two predominant covalent modifications are associated with constitutive heterochromatin throughout the cell cycle: trimethylation of lysine 9 on histone H3 (H3K9me3) and DNA methylation at CpG dinucleotides (Rice *et al.*, 2003; Weber and Schubeler, 2007). Genetic perturbation of the enzymatic machinery responsible for deposition of either of these marks leads to genomic instability, centromeric defects, and gross chromosomal abnormalities (Rice *et al.*, 2003; Weber and Schubeler, 2007). An essential nonhistone component of heterochromatin, heterochromatin protein 1 (HP-1), is conserved throughout the animal and plant kingdoms and localizes to pericentric heterochromatin (Bannister *et al.*, 2001; Lachner *et al.*, 2001). Although the precise architecture of constitutive heterochromatin remains

This article was published online ahead of print in MBoC in Press (http://www.molbiolcell.org/cgi/doi/10.1091/mbc.E11-03-0258) on July 7, 2011.

Address correspondence to: Paul A. Wade (wadep2@niehs.nih.gov).

Abbreviations used: BrdU, bromodeoxyuridine; CTRL, control; FISH, fluorescence in situ hybridization; H3K9me3, histone H3 lysine 9 trimethylation; H3K27me3, histone H3 lysine 27 trimethylation; H4K20me3, histone H4 lysine 20 trimethylation; HP-1, heterochromatin protein 1; MNase, micrococcal nuclease; Sat2, satellite 2; shCHD4, CHD4 short hairpin RNA; shMBD3, MBD3 short hairpin RNA; TSA, trichostatin A.

unknown, it has been proposed that HP-1 dimers stabilize spatially proximal nucleosomes through binding to trimethyl lysine 9 via their chromodomains (Nielsen *et al.*, 2001).

Multiple studies have investigated the role(s) played by chromatin remodeling enzymes in assembly and maintenance of heterochromatin. Both the WSTF-ISWI and ACF-SNF2h complexes localize to pericentric heterochromatin, and perturbation of either results in reduced rates of replication (Collins *et al.*, 2002; Poot *et al.*, 2004). Deletion of Brg1 in murine fibroblasts results in dramatic defects in pericentric heterochromatin, H3K9me3, and aberrant mitoses (Bourgo *et al.*, 2009). Functional deficiencies of the SNF2 family members LSH, DDM1, and ATRX have likewise been associated with defects in pericentric heterochromatin (Gendrel *et al.*, 2002; Xue *et al.*, 2003; Yan *et al.*, 2003).

We previously reported that an additional protein complex containing an SNF2 family ATPase, the Mi-2/NuRD complex, is recruited to a novel nuclear structure in rapidly proliferating B cells, termed NuRD bodies (Helbling Chadwick *et al.*, 2009). These NuRD bodies are localized to pericentric heterochromatin enriched in H3K9me3 specifically during late S phase. Furthermore, NuRD body accumulation is tightly linked to active DNA replication, as well as to chromatin assembly at regions of DNA replication (Helbling Chadwick *et al.*, 2009). In this study, we demonstrate that depletion of the catalytic ATPase subunit CHD4/Mi-2β results in a slow-growth phenotype that is, in part, a manifestation of delayed progression through S phase. In addition, we observe defects in pericentric heterochromatin maintenance and assembly. Our data suggest that incomplete chromatin assembly is sensed by an ATM-dependent intra–S phase checkpoint, resulting in a temporal block to the transition from early to late S phase. These data indicate a critical role for Mi-2β in assembly and/or maintenance of chromatin structure(s) required for proper cell cycle progression.

RESULTS

NuRD complex is required for proper heterochromatin formation

Recent studies propose that Mi-2/NuRD complex is critical for maintaining higher-order chromatin structure and preventing accumulation of double-stranded DNA damage (Pegoraro *et al.*, 2009; Chou *et al.*, 2010; Larsen *et al.*, 2010; Polo *et al.*, 2010; Smeenk *et al.*, 2010). To determine whether NuRD complex may be also functionally relevant to heterochromatin formation, as suggested by its association with replicating DNA (Helbling Chadwick *et al.*, 2009), we depleted two different subunits of NuRD complex in Ramos cells: the ATPase nucleosome remodeling subunit Mi-2β/CHD4 (shCHD4) or MBD3 (shMBD3), which is essential for complex integrity (Kaji *et al.*, 2007). We subsequently evaluated localization of MTA3, a subunit of the NuRD complex. In controls (CTRL), NuRD bodies were seen in ~40% of cells, similar to previous data (Helbling Chadwick *et al.*, 2009). CHD4 knockdown resulted in a decrease of NuRD body formation to ~20% of cells (Figure 1A). In addition, we observed redistribution of MTA3 throughout the nucleus, suggesting that the global chromatin environment is disrupted. Similar to Hutchinson–Gilford progeria syndrome, in which NuRD complex is sequestered at the nuclear lamina, we observed a global loss of H3K9me3 staining in the absence of CHD4 (Figure 1B; Pegoraro *et al.*, 2009). In contrast, there was no change in the localization pattern of another heterochromatic histone modification, histone H4 lysine 20 trimethylation (H4K20me3), indicating that depletion of NuRD complex specifically disrupts localization of trimethylated H3K9 (Supplemental Figure S2A). To rule out that disruption of heterochromatin structure in the absence of CHD4 was unique to Ramos cells, we depleted a second germinal center–like B-cell line, Raji, and saw similar loss of H3K9me3 foci (Supplemental Figure S5).

We hypothesized that depletion of NuRD complex alters pericentric heterochromatin structure at the satellite repeats found on human chromosomes 1, 9, and 16 (Helbling Chadwick *et al.*, 2009). Therefore, we examined gross structure of the megabase block of Satellite 2 (Sat 2) DNA located at pericentric heterochromatin of chromosome 1, using fluorescence in situ hybridization (FISH). The majority of Sat2 structures in CTRL cells show punctate staining, with an equal distribution of signal between foci within the nucleus. In contrast, ~50% of the Sat2 structures in shCHD4 cells scored ($n > 70$) are less compacted and often (~50%) have unequal distribution of signal between foci (Figure 1, C and D). To ensure that the diffuse structures that we observed in shCHD4 cells were not an artifact of imaging, Z-series sections were taken through the nucleus and rendered into a maximum-intensity projected image (Figure 1C, Max Int) with similar results. To determine whether the defects are specific for NuRD body–enriched Sat2 structures, two-color FISH was performed, comparing structures of chromosome 10 alpha satellite repeats (Chr10 α-sat), which do not recruit NuRD complex, to the Sat2 repeats. These repeats remained as discrete foci with equal staining in the absence of CHD4 (Supplemental Figure S2B), demonstrating a failure of appropriate assembly and/or maintenance of higher-order chromatin structure at pericentric heterochromatin.

Although we observed specific effects at pericentric heterochromatin, we hypothesized that Mi-2/NuRD complex may exert a more global influence on chromatin organization. To address this hypothesis, micrococcal nuclease (MNase) digestions were performed to analyze nucleosome structure in shCHD4 cells. Digestion with increasing concentrations of MNase indicated no defects in wrapping of DNA by the histone octamer in bulk chromatin from shCHD4 cells (Figure 2A). However, phosphorylation of KAP1, a marker of global chromatin decondensation, is increased in the absence of CHD4 (Figure 2B; Ziv *et al.*, 2006), suggesting a broad role for CHD4 in some aspect of higher-order chromatin structure but not in assembly or maintenance of normal nucleosome configuration.

CHD4 is required for normal S phase progression

On depletion of CHD4 and MBD3, we observed a slow-growth phenotype at early time points after infection (Figure 3A and Supplemental Figure S1C). However, as cells remain in culture, the growth rate of both shCHD4 and shMBD3 knockdowns mirrors that of CTRLs, suggesting that cells lacking NuRD complex are selected against. Assessment of CHD4 mRNA levels at 7 d after transduction indicated a return to near control levels, supporting the hypothesis that the cells lacking CHD4 are unable to proliferate over many cell divisions (Supplemental Figure S1A, day 7 expression). To further address this, we examined cell viability of cultures 4 and 7 d after infection. Analysis of the sub-G_1 population of cells 4 d after infection revealed that there was a larger proportion of dead cells in the absence of CHD4 compared with CTRL cells (Supplemental Figure S1D, day 4). As the cells remained in culture, the shCHD4 sub-G_1 population decreased and returned to CTRL levels, indicating that cells lacking CHD4 are selected against in culture (Supplemental Figure S1D, day 7).

Early in the time course of depletion (days 4 and 5), we noted a global decrease in markers of G2/M phase, including cyclin B1 and histone H3 serine 10 phosphorylation (H3S10P; Figure 3B), indicating that asynchronous cultures were spending less time in G2/M phase. This result is consistent with increased residence time in G1 as documented recently by several groups for CHD4 depleted cells

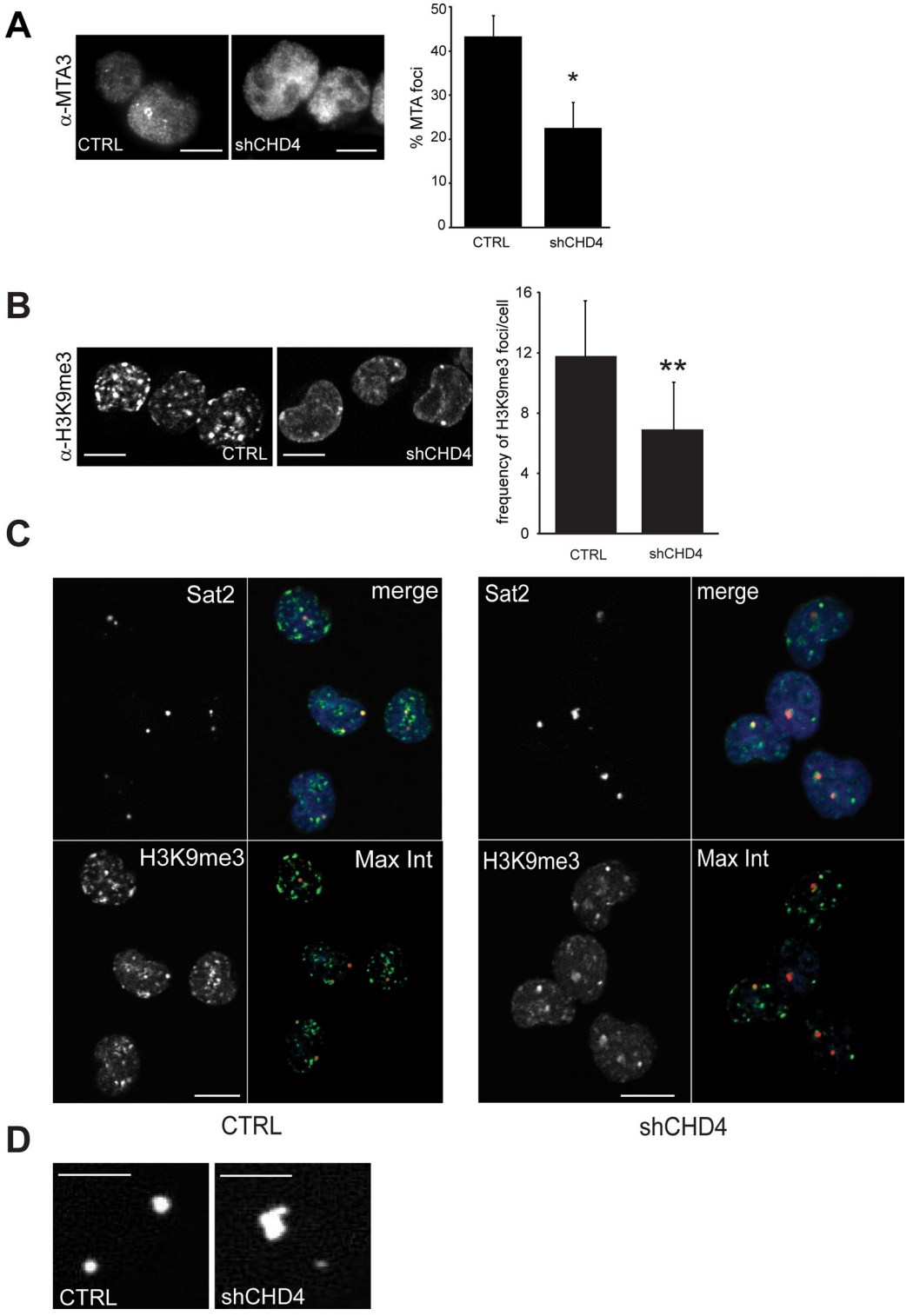

FIGURE 1: Depletion of CHD4 leads to loss of NuRD bodies and defects in pericentric heterochromatin. (A) Left, Ramos cells transduced with either control (CTRL) or CHD4 short hairpin RNA (shCHD4) lentivirus were spun onto slides and stained for MTA3. Right, staining was used to quantify NuRD body formation. Values represent mean ± SD across three independent experiments. *p = 0.005. Scale bars, 10 μm. (B) Left, CTRL and shCHD4 cells were stained for H3K9me3 (n > 200 cells). Right, the number of H3K9me3 foci per cell was quantified using MetaMorph imaging software (see *Materials and Methods*). Values represent mean ± SD across three independent experiments. **p = 0.0001. Scale bars, 10 μm. (C) Representative images of immuno-FISH performed in CTRL and shCHD4-transduced Ramos cells. Cells were stained with H3K9me3 (green) and subsequent fluorescence in situ hybridization using a probe directed against the classic satellite repeat D1Z1 (red). Each panel represents a single plane through the cell, except the final panel, which represents the maximal-intensity projection of the optical sections taken (MAX INT). Total DNA was counterstained with DAPI (blue). Scale bar, 10 μm. (D) Expanded view of Sat2 structures pictured in C. Images represent a single plane acquired by confocal microscopy. Scale bar, 5 μm.

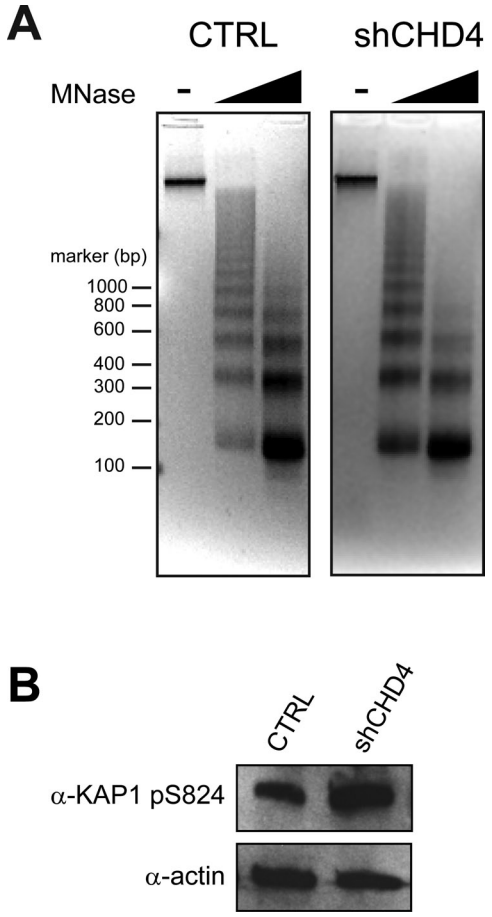

FIGURE 2: Depletion of NuRD complex results in global alterations in chromatin structure. (A) Left, nuclei extracted from CTRL and shCHD4 cells 5 d after transduction were digested with increasing concentrations of micrococcal nuclease (MNase). A total of 1 µg of genomic DNA was analyzed by gel electrophoresis. Positions of DNA ladder are indicated on the left. (B) Western blot analysis of KAP1 phosphorylation 5 d after transduction. Actin was used as a loading control.

(Chou *et al.*, 2010; Larsen *et al.*, 2010; Polo *et al.*, 2010; Smeenk *et al.*, 2010) or with altered kinetics of S phase progression. To examine the effect of depletion of NuRD complex on S phase progression, asynchronous cells lacking CHD4 were labeled with 10 µM BrdU for 15 min and monitored by flow cytometry 4 d after transduction. A moderate increase in the S phase population was observed in shCHD4 cells compared with CTRL cells, indicating a perturbation in S phase (Supplemental Figure S3A). To examine active DNA replication at the individual cell level, bromodeoxyuridine (BrdU)-labeled asynchronous cells were fixed onto slides, stained, and scored as early (I), mid (II), or late (III) S phase as previously described (Wu *et al.*, 2005) (Figure 3C). There was a moderate decrease in the number of shCHD4 cells displaying patterns of mid S phase, suggesting that lack of NuRD complex results in defects in S phase progression (Figure 3C).

To determine the kinetics of S phase progression in the absence of NuRD complex, we synchronized CTRL, shCHD4, and shMBD3 cells at the G1/S boundary, released, and collected cells for analysis of DNA content and replication (by pulse labeling with BrdU prior to collection). At 3 h after release, all transduced cells were able to enter S phase at a similar rate (Supplemental Figure S3, B and C). However, at later time points (4.5 and 6 h), cells lacking CHD4 or MBD3 did not transition to late S phase at the same rate as CTRL cells, indicating that NuRD complex facilitates the transition from mid to late S phase (Figure 3D and Supplemental Figure S3C).

Replication progression can be impeded by an inability to remove histones in front of the replication fork or to load nucleosomes behind the fork (Groth *et al.*, 2007a). A change in nucleosome disassembly/reassembly resulting in replication stress can lead to uncoupling of DNA polymerase from the replicative DNA helicase (Jasencakova *et al.*, 2010). To ascertain the incidence of replication stress in the absence of NuRD complex, we compared localization of Rad51 in CTRL and shCHD4 cells. We observed a significant increase in Rad51 nuclear staining, as well as in formation of nuclear foci, suggesting replication stress and altered fork progression (Figure 3E).

Although completion of DNA replication is delayed, cells lacking NuRD complex are able to complete replication as determined by copy number analysis, demonstrating equivalent abundance of both an early-replicating (glyceraldehyde 3-phosphate dehydrogenase [GAPDH]) and a late-replicating (Sat2) genomic region (Supplemental Figure S3D). These results suggest that although NuRD complex is dispensable for completion of replication, it is critical for normal kinetics of S phase progression.

An ATM-dependent intra–S phase checkpoint is activated in the absence of CHD4

Chromatin structure can be altered by many conditions, including hypotonic growth and treatment with trichostatin A (TSA) or chloroquine (Bakkenist and Kastan, 2003). Such structural defects could result in changes in S phase progression similar to those observed in the absence of NuRD complex. To test this model, we synchronized cells at the G1/S boundary, released into TSA, and monitored progression by flow cytometry. TSA delayed the early to late S phase transition, similar to NuRD complex depletion (Figure 4A and Supplemental Figure S4A). These data predict that cells lacking NuRD complex contain altered chromatin structures that trigger a chromatin quality checkpoint, altering S phase progression. Due to transcriptional repression of ATR in Ramos cells as part of the normal biological program of germinal center B lymphocytes, we focused on components of the ATM signaling pathway (Supplemental Figure S4B). Five days after transduction, an increase in phosphorylated ATM and CHK2 was detected in shCHD4 cells, indicating activation of the ATM signaling pathway (Figure 4, B and C). Furthermore, a marker of S phase stress, histone H3 lysine 56 acetylation (H3K56Ac), was also increased (Figure 4C). This was not due to changes in HDAC activity in the absence of CHD4, as total acetylation of H3 was unchanged (Supplemental Figure S4C). Furthermore, we observed destabilization of CDC25A consistent with altered S phase progression (Figure 4D). In the presence of caffeine, CTRL and shCHD4 cells progressed through S phase at similar rates, confirming that activation of an ATM-dependent checkpoint was responsible for the observed S phase delay (Figure 4E).

We hypothesized that ATM activation was due to altered chromatin structure rather than double-stranded DNA damage. To test this hypothesis, we examined levels of markers of double-strand breaks, γH2AX and phosphorylated serine 14 of histone H2B (H2BS14P), and observed no detectible changes (Supplemental Figure S4, D and E). In addition, inhibition of MRE11, a component of the MRN double-strand break repair complex, had no effect on the slow-proliferation phenotype of CHD4-depleted cells (Supplemental Figure S4F; Dupre *et al.*, 2008). These data support the conclusion that defects in chromatin structure resulting from lack of CHD4

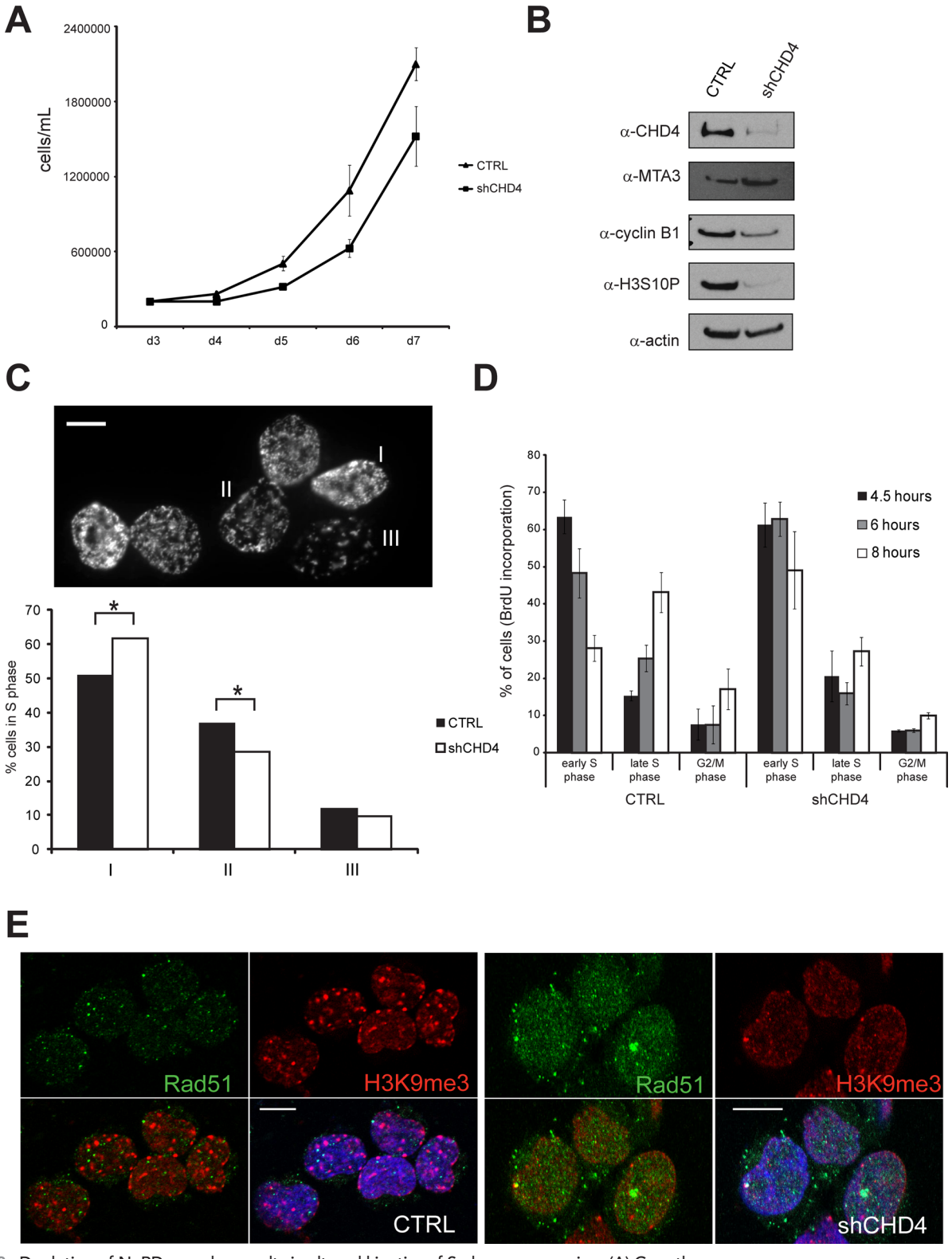

FIGURE 3: Depletion of NuRD complex results in altered kinetics of S phase progression. (A) Growth curves were performed in transduced Ramos cells. Three days after infection, cells were plated at a density of 200,000 cells/ml, and growth was monitored by counting daily until 7 d postinfection (d7). Each time point represents the mean ± SD of three independent experiments. (B) Western blot analysis of the indicated cell cycle markers was performed using Ramos cell extracts collected 5 d after infection. Actin was used as the loading control. (C) Quantification of S phase progression was determined by BrdU patterning and divided into 3 categories (labeled I-III, n > 200). Inset, representative image of CTRL Ramos cells pulsed with BrdU for 15 min. Scale bar, 10 μm. *p = 0.02 (I) and 0.03 (II). (D) Flow cytometric analysis of synchronized CTRL or shCHD4 cells following release from aphidicolin block. Values represent mean ± SD across three independent experiments. (E) Representative images of Rad51 (green) and H3K9me3 (red) immunofluorescence performed in CTRL and shCHD4-transduced Ramos cells (n > 60 cells). Scale bar, 10 μm.

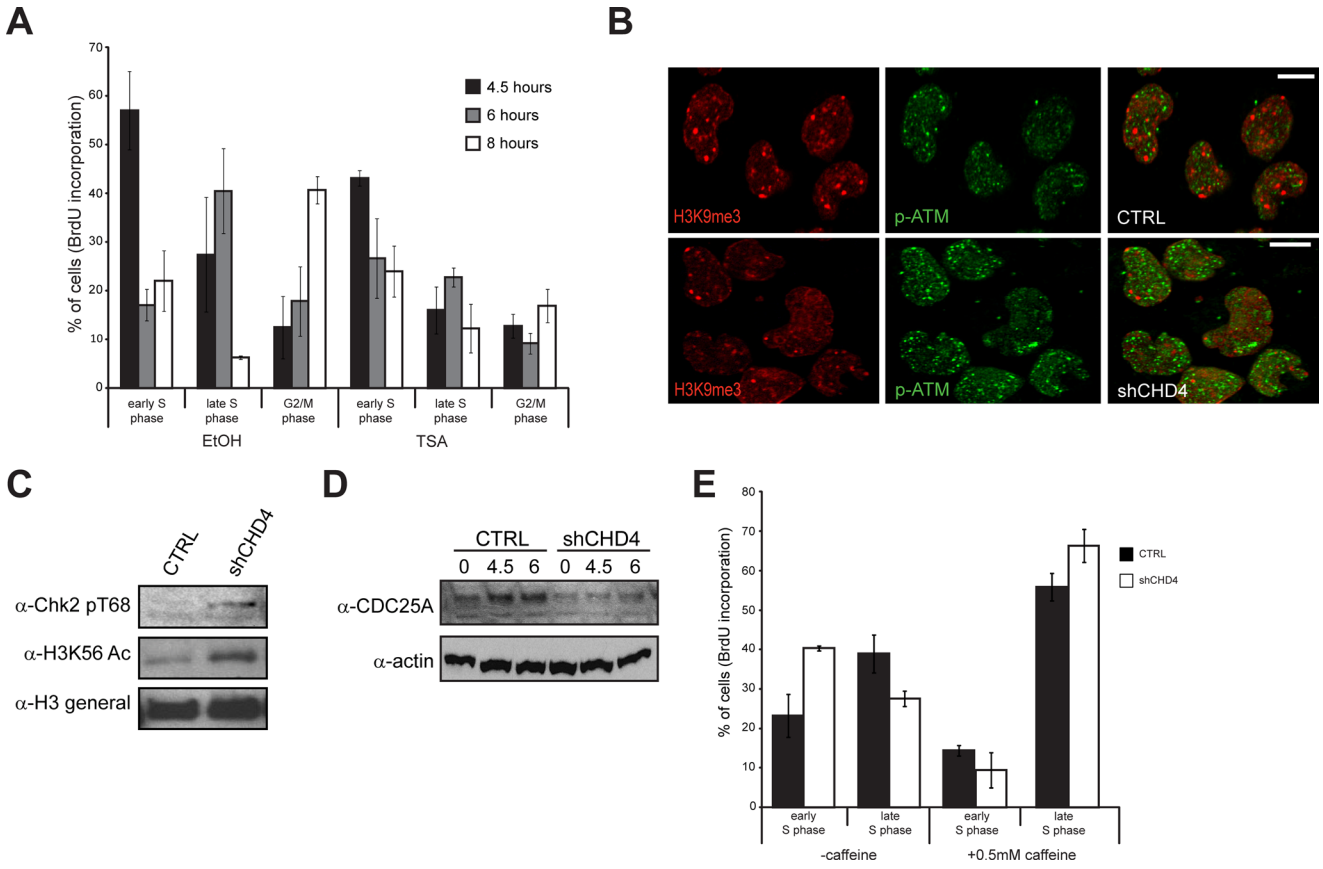

FIGURE 4: Activation of an ATM-dependent intra–S phase checkpoint in cells lacking NuRD complex. (A) Distribution of cells during S phase after treatment with either ethanol (EtOH) or 10 μM TSA. Each value represents the mean ± SD of three independent experiments. (B) Representative images of phosphorylated ATM (green) and H3K9me3 (red) immunofluorescence performed in CTRL and shCHD4-transduced Ramos cells ($n > 75$ cells). Scale bar, 10 μm. (C) Western blot analysis of Chk2 phosphorylation and H3K56Ac. Total histone H3 (H3 general) was used as a loading control. (D) CDC25A protein levels were analyzed in synchronized CTRL and shCHD4 cells following release from aphidicolin block. Actin was used as a loading control. (E) Distribution of transduced cells during S phase after release from aphidicolin block either in the absence (–) or presence (+) of 0.5 mM caffeine.

are sensed by the ATM intra–S phase checkpoint, resulting in delayed transition from early to late S phase (Figure 5).

DISCUSSION

It has been speculated that Mi-2/NuRD complex participates in chromatin assembly due to the unique enzymatic properties of the complex, as well as to its localization to heterochromatin during S phase (Wade *et al.*, 1998; Helbling Chadwick *et al.*, 2009). In this study, we provide evidence that Mi-2/NuRD complex function is critical for replication of higher-order chromatin structure during S phase, as evidenced by aberrant structures at pericentric satellite repeats and accumulation of molecular markers of chromatin decondensation. These chromatin structural defects resulting from loss of CHD4/Mi-2β or MBD3 are manifested in a slow-growth phenotype with delayed S phase progression and activation of an ATM-dependent intra–S phase checkpoint. We observe the activation of ATM and loss of heterochromatin in two different germinal center B-cell lines, Ramos and Raji, indicating that the effects we document are not cell line specific (Supplemental Figure S5). Our data suggest that the initiating signal for checkpoint activation is a physical defect in chromatin structure, implying the presence of a chromatin quality checkpoint in addition to the G2/M chromosome integrity checkpoint (Figure 5).

Chromosomal quality control prior to the completion of DNA synthesis would permit the cell to pause and correct chromatin assembly defects at early replicons prior to initiation of late replication forks. Given the complex nature of higher-order chromatin structures in mammals and the close juxtaposition of unique sequence regions with repetitive DNA, it seems plausible that extensive quality control measures might be used to ensure architectural integrity and appropriate functional partitioning of the genome. Manipulation of components of both chromatin assembly machinery and chromatin-modifying enzymes results in defects in S phase progression, activation of intra–S phase checkpoint, and changes in chromatin structure, supporting our hypothesis that improper histone modifications and alterations in chromatin structure are detrimental (Bakkenist and Kastan, 2003; Ye *et al.*, 2003; Bhaskara *et al.*, 2008; Quivy *et al.*, 2008). Furthermore, the presence of multiple signaling pathways suggests an intimate relationship between chromatin assembly and cell cycle control, including mediation of Asf1 function by both Chk2 and the Tlk1 signaling pathway (Emili *et al.*, 2001; Hu *et al.*, 2001; Groth *et al.*, 2003). Using an ATM-dependent pathway to survey alterations in chromatin structure could serve as an efficient mechanism to prevent fork progression in the absence of appropriate chromatin assembly, which could potentially leave DNA vulnerable to rearrangements, nuclease degradation, or formation

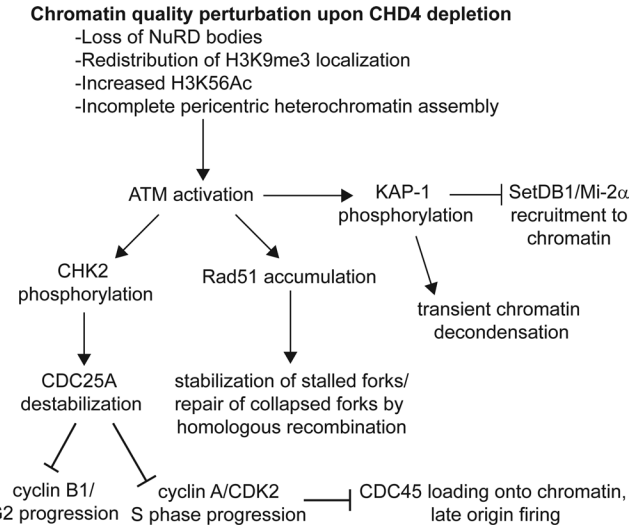

FIGURE 5: Mi-2/NuRD complex depletion in germinal center B cells leads to alterations in chromatin, checkpoint activation, and delayed progression through S phase. Disruption of pericentric heterochromatin higher-order structure results in activation of ATM, as well as downstream components of the intra–S phase checkpoint. This signaling pathway delays S phase progression by destabilizing CDC25A to prevent late origin firing, blocking cyclin B1 production to prevent progression into G2 phase, and accumulating nuclear Rad51, which stabilizes stalled or damaged forks and blocks further replication.

of secondary structures that can be read as DNA damage (Lambert and Carr, 2005; Groth *et al.*, 2007a, 2007b; Quivy *et al.*, 2008).

Multiple SNF2 superfamily ATPase enzymes have been documented to have similar functions in chromatin remodeling and have been implicated as critical to the integrity of pericentric heterochromatin (Collins *et al.*, 2002; Gendrel *et al.*, 2002; Xue *et al.*, 2003; Yan *et al.*, 2003; Poot *et al.*, 2004; Bourgo *et al.*, 2009; Cohen *et al.*, 2010; Cohet *et al.*, 2010). This apparent paradox could result from multiple scenarios that are not mutually exclusive. It is conceivable that different cell types use different combinations of SNF2 ATPases in the process of chromatin maturation at these structures, depending on the local chromatin environment. Multiple histone modifications, as well as patterns of DNA methylation, are critical for defining specific types of heterochromatin. Data from our previous work describe three cell-type-specific subclasses of pericentric heterochromatin as defined by enrichment of H3K9me3, H3K27me3, and H4K20me3 alone or in combination (Helbling Chadwick *et al.*, 2009). These variations in chromatin composition could result in recruitment of different SNF2 ATPases. Alternatively, the process of replicating pericentric heterochromatin may be staged, with each stage requiring a different ATPase subunit. Studies of the ISWI complex in S phase progression have demonstrated that SNF2H, ACF1, and WSTF are critical for decondensation of heterochromatin ahead of the replication fork, whereas our current data are more compatible with a direct role for CHD4 in assembly of higher-order structure(s) following fork progression (Figure 5; Collins *et al.*, 2002; Poot *et al.*, 2004; Helbling Chadwick *et al.*, 2009).

Maintenance of genome integrity is an essential process facilitated in eukarya by the nucleoprotein structures of chromatin. Multiple disease states result from mutation or aberrant function of enzymes dedicated to formation and/or maintenance of normal chromatin architecture, including the Mi-2/NuRD complex (Sillibourne *et al.*, 2007; Pegoraro *et al.*, 2009; Chou *et al.*, 2010; Cohet *et al.*, 2010; Larsen *et al.*, 2010; Misteli, 2010; Polo *et al.*, 2010; Smeenk *et al.*, 2010). Our results highlight the quality control processes engaged to monitor appropriate chromatin assembly to ensure that cells stably maintain their genomes.

MATERIALS AND METHODS

Cell culture

Ramos and Raji cells were purchased from the American Type Culture Collection (Rockville, MD) and maintained in RPMI 1640 medium (Life Technologies, Carlsbad, CA) supplemented with 10% fetal bovine serum (FBS). 293T lentiviral packaging cells were maintained in DMEM/F12 medium (Life Technologies) supplemented with 10% FBS.

Short hairpin RNA–mediated depletion of CHD4 and MBD3

Generation of lentivirus was performed as previously described (Lai *et al.*, 2010), using the following vectors: pGIPZ shCHD4 (V2LHS_14657), shMBD3 (V3LHS_392211), and pGIPZ empty (RHS4349) (Open Biosystems, Thermo Biosystems, Huntsville, AL). Fluorescence-activated cell sorting (FACS) based on green fluorescent protein (GFP) intensity was used (FACSVantage with Digital Option; BD Biosciences, San Diego, CA).

Western analysis

Total protein was extracted from GFP-positive cells using lysis buffer (8 M urea, 1% SDS, 0.125 M Tris, pH 6.8), and phosphorylated proteins were enriched using a PhosphoProtein Purification Kit (Qiagen, Valencia, CA). Total protein extract was analyzed by resolving 10 μg of protein or 50 μg of phosphoprotein lysate on SDS–PAGE gels and immunoblotted using the following antibodies: CHD4 (A301-081A; Bethyl Laboratories, Montgomery, TX), MBD3 (sc-9402; Santa Cruz Biotechnology, Santa Cruz, CA), actin (MAB1501; Chemicon, Millipore, Billerica, MA), ATR (sc-1887; Santa Cruz Biotechnology), H3 general (ab1791; Abcam, Cambridge, MA), H3 acetylation (06-599; Upstate, Millipore), γH2AX (05-636; Upstate, Millipore), H3K56Ac (39281; Active Motif, Carlsbad, CA), MTA3, cyclin B1 (sc-594, Santa Cruz Biotechnology), H3S10P (sc-8656-R; Santa Cruz Biotechnology), phospho-CHK2 (2197, Cell Signaling Technology, Beverly, MA), phospho-KAP-1 (S824, A300-767A-1; Bethyl Laboratories), CDC25A (ab2357; Abcam,), H2BS14P (07-191; Upstate, Millipore), and H2B general (07-371, Upstate, Millipore).

Immunofluorescence, fluorescence in situ hybridization, and imaging

Immunofluorescence and immuno-FISH were performed as previously described (Helbling Chadwick *et al.*, 2009), using the following antibodies and probes: H3K9me3 (07-523; Millipore), MTA3 (Fujita *et al.*, 2004), BrdU (347580; BD Biosciences), H3S10P (sc-8656-R; Santa Cruz Biotechnology), H4K20me3 (39180; Active Motif), Rad51 (ab213; Abcam), P-ATM (S1981) (10H11.E12; Cell Signaling Technology), Classical Satellite (D1Z1) (LPE-001; Rainbow Scientific, Windsor, CT), and Chromosome 10 alpha satellite (LPE-010; Rainbow Scientific). To expose BrdU antigens for detection of actively replicating genomic regions, fixed and blocked cells were immersed in 4 N HCl for 10 min, followed by extensive washing in phosphate-buffered saline prior to the addition of BrdU antibody.

Images were collected on a Zeiss Axiovert 200 imaging system equipped with an Axiocam MR digital camera controlled by

AxioVision software (Zeiss, Thornwood, NY). Confocal images were collected on a Zeiss LSM 510 UV laser scanning confocal microscope controlled by Zeiss LSM software. Maximum-intensity projections were derived from Z-series images taken at 1-µm steps and rendered around a single x-axis plane. Images were analyzed using Photoshop CS2 (Adobe, San Jose, CA) and Zeiss LSM software. H3K9me3 and H4K20me3 foci analysis was performed using MetaMorph imaging software (version 7.7.1; Molecular Devices, Downington, PA) to count the number of nuclei in an image in addition to the number of H3K9me3 or H4K20me3 foci in each cell. First nuclei were counted with the Integrated Morphology Analysis feature using a threshold (>50 units) to separate each nucleus. In instances in which multiple nuclei overlapped, manual separation was performed with the cut tool. The threshold was then reset, and a morphological TopHat filter (100 pixels^2) was applied to identify the heterochromatin. Before measuring the number of heterochromatin spots by "integrated morphometry," a low threshold (<10 units) was applied to filter low-intensity noise. Log data were then transferred to Excel sheets (Microsoft, Redmond, WA). Student's *t* tests were used to determine statistical significance of all images analyzed.

Cell synchronization and FACS analysis

Two days after transduction, Ramos cells were synchronized as previously described (Helbling Chadwick *et al.*, 2009). After synchronization, cells were released into medium either in the presence or absence of 0.5 mM caffeine or 10 µM TSA (Sigma-Aldrich, St. Louis, MO). At each time point, cells were pulsed with 10 µM BrdU for 15 min, fixed, and stained using the APC BrdU Flow Kit (BD Biosciences). Cells were analyzed using the BD LSR II Flow Cytometer System. Analysis of flow data were performed using Flowjo software (TreeStar, Ashland, OR).

Nucleic acid extraction

Total RNA was extracted from GFP-positive cells 5 d after transduction using the RNeasy Mini Kit (Qiagen). cDNA was synthesized as described (Fujita *et al.*, 2004). Expression analysis of NuRD complex members was performed using Quantitect primer assays (Qiagen): MTA3 (QT00064988), CHD4 (QT00025522), CHD3 (QT00007063), MBD2 (QT00007084), MBD3 (QT00035252), and GAPDH (QT01192646). Total genomic DNA was extracted from GFP-positive cells 7 d after transduction using the DNeasy Mini Kit (Qiagen). Copy-number analysis was performed as described (Quivy *et al.*, 2008), using the following primer sets: Satellite 2, CATCGAATGGAAATGAAAGGAGTC and ACCATTGGATGATTGCAGTCAA; GAPDH, GCCCCCGGTTTCTATAAATTG and GGCGACGCAAAAGAAGATG

MNase digestion

Cells were incubated in nuclear isolation buffer (150 mM NaCl, 10 mM 4-(2-hydroxyethyl)-1-piperazineethanesulfonic acid, pH 7.5, 1.5 mM $MgCl_2$, 10 mM KCl, 0.5% Nonidet P-40, 0.5 mM dithiothreitol) at 4°C to release nuclei. Nuclei were resuspended in MNase digestion buffer (0.32 M sucrose, 50 mM Tris-HCl, pH 7.4, 4 mM $MgCl_2$, 1 mM $CaCl_2$) to a final concentration of 1 µg/ml as determined by A_{260}. Amounts of 0.01, 0.05, 0.1, and 0.5 µg/ml MNase were added, and nuclei were digested for 5 min at 37°C before quenching with 10 mM EDTA. Amounts of 0.02% SDS, 1 µg of proteinase K, and 1 µg of RNase A were added prior to phenol extraction and ethanol precipitation of genomic DNA. A total of 1 µg of DNA was fractionated by agarose electrophoresis.

ACKNOWLEDGMENTS

We gratefully acknowledge C. J. Tucker, Agnus Janoshazi, and the Fluorescence Microscopy and Imaging Center, National Institute of Environmental Health Sciences, for assistance with microscopy and quantitation of images. We thank Carl Bortner, Maria Sifre, and the Flow Cytometry Center, National Institute of Environmental Health Sciences, for assistance with flow cytometry. This work was substantially improved by critical comments on the manuscript and discussion with Karen Adelman, Aleksandra Adomas, Archana Dhasarathy, Guang Hu, and Anne Lai. This work was supported by the Intramural Research Program of the National Institute of Environmental Health Sciences, National Institutes of Health (Project Z01ES101965 to P.A.W.).

REFERENCES

Bakkenist CJ, Kastan MB (2003). DNA damage activates ATM through intermolecular autophosphorylation and dimer dissociation. Nature 421, 499–506.

Bannister AJ, Zegerman P, Partridge JF, Miska EA, Thomas JO, Allshire RC, Kouzarides T (2001). Selective recognition of methylated lysine 9 on histone H3 by the HP1 chromo domain. Nature 410, 120–124.

Bhaskara S, Chyla BJ, Amann JM, Knutson SK, Cortez D, Sun ZW, Hiebert SW (2008). Deletion of histone deacetylase 3 reveals critical roles in S phase progression and DNA damage control. Mol Cell 30, 61–72.

Bourgo RJ *et al.* (2009). SWI/SNF deficiency results in aberrant chromatin organization, mitotic failure, and diminished proliferative capacity. Mol Biol Cell 20, 3192–3199.

Chou DM, Adamson B, Dephoure NE, Tan X, Nottke AC, Hurov KE, Gygi SP, Colaiacovo MP, Elledge SJ (2010). A chromatin localization screen reveals poly (ADP ribose)-regulated recruitment of the repressive polycomb and NuRD complexes to sites of DNA damage. Proc Natl Acad Sci USA 107, 18475–18480.

Cohen SM, Chastain PD 2nd, Rosson GB, Groh BS, Weissman BE, Kaufman DG, Bultman SJ (2010). BRG1 co-localizes with DNA replication factors and is required for efficient replication fork progression. Nucleic Acids Res 38, 6906–6919.

Cohet N, Stewart KM, Mudhasani R, Asirvatham AJ, Mallappa C, Imbalzano KM, Weaver VM, Imbalzano AN, Nickerson JA (2010). SWI/SNF chromatin remodeling enzyme ATPases promote cell proliferation in normal mammary epithelial cells. J Cell Physiol 223, 667–678.

Collins N, Poot RA, Kukimoto I, Garcia-Jimenez C, Dellaire G, Varga-Weisz PD (2002). An ACF1-ISWI chromatin-remodeling complex is required for DNA replication through heterochromatin. Nat Genet 32, 627–632.

Dupre A *et al.* (2008). A forward chemical genetic screen reveals an inhibitor of the Mre11-Rad50-Nbs1 complex. Nat Chem Biol 4, 119–125.

Emili A, Schieltz DM, Yates JR 3rd, Hartwell LH (2001). Dynamic interaction of DNA damage checkpoint protein Rad53 with chromatin assembly factor Asf1. Mol Cell 7, 13–20.

Fujita N, Jaye DL, Geigerman C, Akyildiz A, Mooney MR, Boss JM, Wade PA (2004). MTA3 and the Mi-2/NuRD complex regulate cell fate during B lymphocyte differentiation. Cell 119, 75–86.

Gendrel AV, Lippman Z, Yordan C, Colot V, Martienssen RA (2002). Dependence of heterochromatic histone H3 methylation patterns on the *Arabidopsis* gene DDM1. Science 297, 1871–1873.

Groth A, Corpet A, Cook AJ, Roche D, Bartek J, Lukas J, Almouzni G (2007a). Regulation of replication fork progression through histone supply and demand. Science 318, 1928–1931.

Groth A, Lukas J, Nigg EA, Sillje HH, Wernstedt C, Bartek J, Hansen K (2003). Human Tousled like kinases are targeted by an ATM- and Chk1-dependent DNA damage checkpoint. EMBO J 22, 1676–1687.

Groth A, Rocha W, Verreault A, Almouzni G (2007b). Chromatin challenges during DNA replication and repair. Cell 128, 721–733.

Helbling Chadwick L, Chadwick BP, Jaye DL, Wade PA (2009). The Mi-2/NuRD complex associates with pericentromeric heterochromatin during S phase in rapidly proliferating lymphoid cells. Chromosoma 118, 445–457.

Henikoff S (2000). Heterochromatin function in complex genomes. Biochim Biophys Acta 1470, O1–O8.

Hu F, Alcasabas AA, Elledge SJ (2001). Asf1 links Rad53 to control of chromatin assembly. Genes Dev 15, 1061–1066.

Jasencakova Z, Scharf AN, Ask K, Corpet A, Imhof A, Almouzni G, Groth A (2010). Replication stress interferes with histone recycling and predeposition marking of new histones. Mol Cell 37, 736–743.
Kaji K, Nichols J, Hendrich B (2007). Mbd3, a component of the NuRD co-repressor complex, is required for development of pluripotent cells. Development 134, 1123–1132.
Lachner M, O'Carroll D, Rea S, Mechtler K, Jenuwein T (2001). Methylation of histone H3 lysine 9 creates a binding site for HP1 proteins. Nature 410, 116–120.
Lai AY *et al*. (2010). DNA methylation prevents CTCF-mediated silencing of the oncogene BCL6 in B cell lymphomas. J Exp Med 207, 1939–1950.
Lambert S, Carr AM (2005). Checkpoint responses to replication fork barriers. Biochimie 87, 591–602.
Larsen DH *et al*. (2010). The chromatin-remodeling factor CHD4 coordinates signaling and repair after DNA damage. J Cell Biol 190, 731–740.
Meselson M, Stahl FW (1958). The replication of DNA in *Escherichia coli*. Proc Natl Acad Sci USA 44, 671–682.
Misteli T (2010). Higher-order genome organization in human disease. Cold Spring Harb Perspect Biol 2, a000794.
Nielsen AL, Oulad-Abdelghani M, Ortiz JA, Remboutsika E, Chambon P, Losson R (2001). Heterochromatin formation in mammalian cells: interaction between histones and HP1 proteins. Mol Cell 7, 729–739.
Pegoraro G, Kubben N, Wickert U, Gohler H, Hoffmann K, Misteli T (2009). Ageing-related chromatin defects through loss of the NURD complex. Nat Cell Biol 11, 1261–1267.
Polo SE, Kaidi A, Baskcomb L, Galanty Y, Jackson SP (2010). Regulation of DNA-damage responses and cell-cycle progression by the chromatin remodelling factor CHD4. EMBO J 29, 3130–3139.
Poot RA, Bozhenok L, van den Berg DL, Steffensen S, Ferreira F, Grimaldi M, Gilbert N, Ferreira J, Varga-Weisz PD (2004). The Williams syndrome transcription factor interacts with PCNA to target chromatin remodelling by ISWI to replication foci. Nat Cell Biol 6, 1236–1244.
Quivy JP, Gerard A, Cook AJ, Roche D, Almouzni G (2008). The HP1-p150/CAF-1 interaction is required for pericentric heterochromatin replication and S-phase progression in mouse cells. Nat Struct Mol Biol 15, 972–979.
Rice JC, Briggs SD, Ueberheide B, Barber CM, Shabanowitz J, Hunt DF, Shinkai Y, Allis CD (2003). Histone methyltransferases direct different degrees of methylation to define distinct chromatin domains. Mol Cell 12, 1591–1598.
Sillibourne JE, Delaval B, Redick S, Sinha M, Doxsey SJ (2007). Chromatin remodeling proteins interact with pericentrin to regulate centrosome integrity. Mol Biol Cell 18, 3667–3680.
Smeenk G, Wiegant WW, Vrolijk H, Solari AP, Pastink A, van Attikum H (2010). The NuRD chromatin-remodeling complex regulates signaling and repair of DNA damage. J Cell Biol 190, 741–749.
Wade PA, Jones PL, Vermaak D, Wolffe AP (1998). A multiple subunit Mi-2 histone deacetylase from *Xenopus laevis* cofractionates with an associated Snf2 superfamily ATPase. Curr Biol 8, 843–846.
Weber M, Schubeler D (2007). Genomic patterns of DNA methylation: targets and function of an epigenetic mark. Curr Opin Cell Biol 19, 273–280.
Wu R, Terry AV, Singh PB, Gilbert DM (2005). Differential subnuclear localization and replication timing of histone H3 lysine 9 methylation states. Mol Biol Cell 16, 2872–2881.
Xue Y, Gibbons R, Yan Z, Yang D, McDowell TL, Sechi S, Qin J, Zhou S, Higgs D, Wang W (2003). The ATRX syndrome protein forms a chromatin-remodeling complex with Daxx and localizes in promyelocytic leukemia nuclear bodies. Proc Natl Acad Sci USA 100, 10635–10640.
Yan Q, Huang J, Fan T, Zhu H, Muegge K (2003). Lsh, a modulator of CpG methylation, is crucial for normal histone methylation. EMBO J 22, 5154–5162.
Ye X, Franco AA, Santos H, Nelson DM, Kaufman PD, Adams PD (2003). Defective S phase chromatin assembly causes DNA damage, activation of the S phase checkpoint, and S phase arrest. Mol Cell 11, 341–351.
Ziv Y, Bielopolski D, Galanty Y, Lukas C, Taya Y, Schultz DC, Lukas J, Bekker-Jensen S, Bartek J, Shiloh Y (2006). Chromatin relaxation in response to DNA double-strand breaks is modulated by a novel ATM- and KAP-1 dependent pathway. Nat Cell Biol 8, 870–876.